Journal of Thermal Analysis and Calorimetry, Vol. 70 (2002) 633–649

MOLECULAR MOBILITY IN POLYMERS STUDIED WITH THERMALLY STIMULATED RECOVERY
I. Experimental procedures and data treatment

N. M. Alves[1], *J. F. Mano*[1*] *and J. L. Gómez Ribelles*[2]

[1]Polymer Engineering Department, University of Minho, Campus of Azurém, 4800-058 Guimarães, Portugal
[2]Center for Biomaterials and Dept. of Applied Thermodynamics, Universidad Politécnica de Valencia, P. O. Box 22012, E-46071 Valencia, Spain

(Received January 15, 2002; in revised form April 15, 2002)

Abstract

Thermally stimulated recovery, TSR, like as thermally stimulated depolarisation currents, is a suitable technique that allows for the study of conformational mobility in polymeric systems. Due to its relatively low equivalent frequency and transient nature, the viscoelastic data obtained from this technique are complementary to conventional dynamic mechanical analysis (DMA). In this work TSR-like experiments, including TSR, thermally stimulated creep and thermal sampling (TS) experiments were carried out in the same commercial DMA equipment, allowing for the direct comparison of the data. Some advises for running TSR experiments are presented, such as the need of performing blank experiments and temperature calibrations. The analysis of the data to obtain the thermokinetic parameters of TS experiments is revised. In particular, from the direct fitting of the data, it is reported a tendency for a linear relationship between the pairs of values of (E_a,log τ_0) that best adjust any TS single experiment. It is concluded that the usual equation for describing TS experiments possesses an intrinsic compensation between these two thermokinetic parameters.

Keywords: glass transition, thermo-mechanical behaviour, TSR, viscoelasticity

Introduction

Relaxation processes and the underlying molecular motions of polymers have been widely investigated due to the fact that they allow to establish correlations between their macroscopic properties and the corresponding molecular structure. For example, the onset of large-scale cooperative mobility at the molecular level associated with the glass transition is related with drastic changes in many physical properties [1]. Moreover, lower temperature secondary relaxations have influence on some important properties such as impact strength [2, 3].

* Author for correspondence: E-mail: jmano@dep. uminho.pt

1418–2874/2002/ $ 5.00
Akadémiai Kiadó, Budapest

A variety of spectroscopic techniques have been used to study relaxational phenomena in polymeric systems [4]. Among them, those using cyclic electric or mechanical stimulus are widely used. In those cases, the sample is subjected to an electric field or to a stress (or strain), responding with a polarisation or a strain (or stress) that is measured as a function of frequency or temperature. The use of a dynamical stimulus has the advantage of leading to a response that can be separated into two components, related with the components in and out of phase with the excitation. The use of these procedures are advantageous for the case of polymeric systems due to the inelastic character of the molecular mobility usually observed. In such dynamic experiments the use of relatively low frequencies is avoided because of the long data collection time. In fact, one must measure the sample's response over a segment of the period of the excitation. To reach lower equivalent frequency ranges (for example below 0.01 Hz) transient techniques are often used. Here a static stimulus is imposed and the response is monitored *vs*. time. In other kind of transient techniques the response is monitored while the sample is subjected to a temperature program, usually a heating at a constant rate. The thermally stimulated depolarisation technique (TSDC) in which the polarisation release of a previously poled sample is investigated [5, 6] is the most used. The corresponding mechanical equivalent technique, usually called thermally stimulated creep (TSCreep), or thermally stimulated recovery (TSR) has also been used, with the advantage of giving direct viscoelastic information and the possibility of being used in non-polar systems [7–17]. A similar technique called creep rate spectroscopy has also been reported [18, 19].

In a 'global' TSR experiment a static stress is imposed to the sample at a temperature (T_σ) higher than the temperature location of the relaxation under study. Thus, in the resulting strain all molecular processes are involved because all characteristic times, $\tau(T_\sigma)$, are small enough to quickly respond to the mechanical stimulus. During this creep process the sample is cooled down to a lower temperature (T_0), at which the characteristic times are such that any recovery process could not occur at a reasonable time scale. During a controllable heating process those times are progressively reduced and when they reach sufficiently small values, that will depend on the equivalent frequency of the technique, the recovery process may be observed as a sudden decrease of the $\varepsilon(T)$ line (or peaks in a $d\varepsilon/dT$ plot). The different translational/rotational mobility processes of the material may be then investigated by observing the $d\varepsilon/dT$ peaks in the temperature axis.

The TSR technique offers the interesting possibility of decompose a complex process, characterised by a distribution of characteristic times, into narrow distributions of relaxations, enabling analysis of the fine structure of the TSR global spectra [7–9, 20, 21]. Each of such elementary components are usually considered as thermally activated simple processes in which the kinetic features are characterised by an activation energy and a pre-exponential factor. This procedure, called thermal sampling (TS) or thermal windowing will be described in the experimental section.

The equivalent frequencies associated with such thermostimulated techniques are usually in the range from 10^{-2} to 10^{-3} Hz [22], which are relatively low when compared to the usual frequencies accessed in dynamic experiments. This time scale is

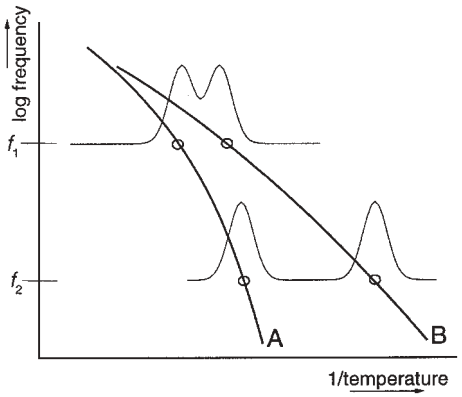

Fig. 1 Arrhenius diagram of a system presenting two relaxation processes (A and B with higher and lower activation energies, respectively). The isochronal response (fixed frequency) of the two processes in the temperature axis is given by thinner lines with the peaks. The peaks corresponding to the two processes are more separated if the measurements are performed at lower frequencies (in that case f_2, with respect to f_1)

connected with the heating rate, that is the relevant experimental variable on TSR. The low frequency of the TSR technique is expected to enhance the resolution of the different relaxation processes. Figure 1 justifies such statement, displaying an example of a system with two possible processes. The lower temperature processes usually have lower activation energies (or lower absolute derivatives of log$f$ *vs*. $1/T$ in the case of non-thermally activated processes, such as the glass transition relaxation). Therefore response peaks (such as those seen in E'' *vs*. T or $d\varepsilon/dT$ *vs*. T plots) are found to be more separated at lower frequency tests.

The low frequency character of TSR experiments, due to its transient nature, or the possibility of decompose a complex process with the TS procedure makes this technique a complementary tool of the classical dynamic mechanical analysis (DMA) experiments. In this work, we pretend to explore the possibility of performing TSR-type experiments in a commercial DMA equipment. This would allow for the comparison between such results and the dynamic data obtained in the same experimental environment. The DMA apparatus used in this work permits to use different mechanical modes such as three-point bending, dual or single cantilever, extension and compression; this allows to carry out experiments in a variety of stress environments. In fact most of the reported studies on TSR-like techniques used torsion stresses; to our knowledge only one study presented data obtained in flexion [23].

Due to the fact that TSR-type measurements are carried out in heating, there is a difference between the temperature read by the thermocouple and the real temperature of the sample. In this work special attention is given to this problem.

Experimental

Methods and apparatus

Both TSR and DMA experiments were carried out using a DMA7e Perkin Elmer apparatus with a controlled cooling device. High purity helium at constant flow rate was used for purging the sample environment during the experiments, allowing a better thermal contact between the furnace and the sample.

The creep/recovery mode of the apparatus allows to apply simultaneously static stresses and temperature programs. Three kinds of thermally stimulated experiments can be performed.

1) Thermally stimulated recovery experiments TSR: the sample was cooled to a temperature T_σ which is above the temperature range of the studied relaxation processes. During a creep period (t_σ) the sample is subjected to a static mechanical stress and then cooled down to a temperature T_0, where the mechanical field is removed. During a controlled heating the recovery of the sample's strain is monitored as a function of temperature. The complete scheme of this type of experiment is shown in Fig. 2a.

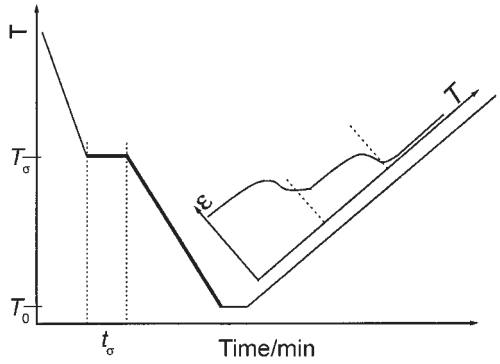

Fig. 2a Scheme of a global TSR experiment. The thicker lines in the *T vs*. *t* plot correspond to experimental steps where a static stress was applied

2) Thermally stimulated creep experiment TSCreep: the strain of the sample, subjected to a static stress during a controlled heating, is monitored as a function of temperature (Fig. 2b). The sample was previously cooled from a temperature well above the temperature range of the studied processes to erase any thermomechanical history.

3) Thermal sampling experiments (TS): the mechanical stress was applied only in a narrow temperature range within the temperature region where the global process appears. A typical TS experiment is schematically shown in Fig. 2c and may be described as follows: i) a static stress σ_0 was applied at T_σ during a time period t_σ (T_σ varies from experiment to experiment in the region of the global process); ii) the sam-

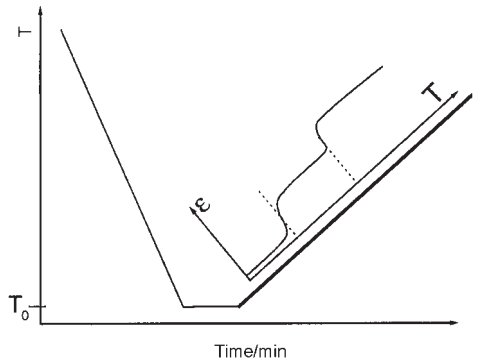

Fig. 2b Scheme of a global TSCreep experiment. A static stress is applied during the final heating step (thicker line in the *T vs. t* representation)

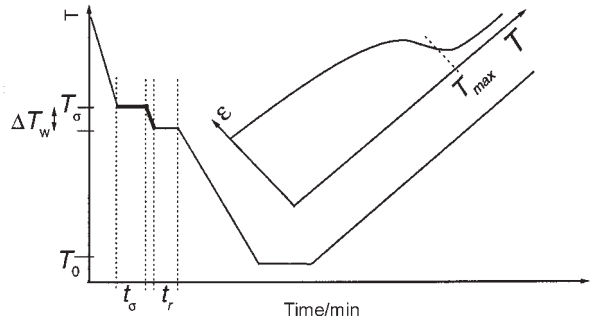

Fig. 2c *T–t* plot of a typical TS experiment. A static stress was applied during the isothermal stage at T_σ and also during the cooling down to T_σ–ΔT_w (thicker lines). Typical values of the experimental variables t_σ~5 min, ΔT_w~3°C, t_r~2 min, β~4°C min^{-1}. T_{max} is the inflexion temperature of ε(*T*)

ple was quenched to $T_r=T_\sigma-\Delta T_w$ with the mechanical field on; iii) the stress was removed and the mechanical strain is allowed to recover during a period of time t_r; iv) the sample was quenched to T_0, well below the temperature region of the global process (say 50°C below T_σ); and v) the position of the probe tip was monitored during a controlled heating (typically 4°C min^{-1}), from T_0 up to a final temperature well above T_σ. The processes recovered in this heating step were those having retardation times in the range from ~100 to ~1000 s at T_σ.

Temperature calibration

There are several factors that cause a difference between the temperature read by the sensor and the true temperature of the sample. First, in non-isothermal experiments, there is a temperature gradient between the sensor and the sample due to thermal fluxes related to the change of temperature inside the furnace. Even in isothermal

conditions, there are thermal fluxes due to the different temperatures in the different points inside the furnace, that depend on the temperature control, the geometry of the furnace, or the helium flux. One can also have intrinsic errors in the sensor's reading. Finally, mainly in non-isothermal conditions, the own thermal resistance of the sample leads to a distribution of temperatures in the different points of the sample, principally through the sample's thickness.

Therefore the use of a temperature calibration routine is important in TSR, with reinforced relevance by the fact that the measurements are carried out in non-isothermal conditions. Traditionally, temperature calibration in dynamic mechanical analysis and thermomechanical analysis experiments uses the instruments in a penetration mode, in which the displacement of a probe tip imposing a static force into a small standard metallic sample is monitored during a heating at a specific rate. The onset of the probe displacement curve is compared with the known melting point of the standard used. More details about this calibration procedure, in which different types of apparatus were tested, can be found elsewhere [24, 25]. As the temperature lag depends on the mechanical mode used (extension, flexural…) one should adopt different procedures depending on the device used. For tensile experiments in fibres, Riesen and Schawe attached a small indium pellet in the fibre and the melting of the metal could be detected by the length's change of the fibre [26].

In this work we used a different concept for flexural and tensile experiments, also using the apparatus in a penetration mode.

i) For the flexural experiments: the metallic standard piece is placed in the top-centre of a plastic piece with similar geometry of the sample that one pretends to study. This plastic piece is placed, like as any sample, over the edges of the flexural platform (Fig. 3, bottom right). The plastic that one should use must have a T_g above the melting point of the standard metal so that no geometry changes occur in it. A piece of polyimide was used in this work. Usually metallic probe tips are used to apply the mechanical forces to the sample. In this calibration procedure, the used probe tip was made of teflon in order to minimise thermal fluxes between the standard and the metallic round-bar that links the probe tip to the upper electronic/mechanical system of the apparatus. With this method we probe the temperature just in the surface of the sample.

ii) For the tensile experiments: another procedure is proposed where the temperature is probed in the centre region of the sample studied. In this arrangement the standard is hold by a plastic platform between the two clamps. Again the used plastic must have a sufficiently high T_g. Semicrystalline PEEK was used in this work, with $T_g \approx 144$°C and $T_m \approx 335$°C. Two PEEK strips (about 0.2 mm thickness), with approximately half of the length of the sample under study were attached in the two clamps (Fig. 3, top right). A small PEEK platform was glued at the top of the bottom strip, to support the metallic standard, and the top strip was used as the probe tip (Fig. 3, top right). This procedure pretended to simulate the same thermal environment of a tensile test and measures the temperature near the surface of the half-length of a tensile sample.

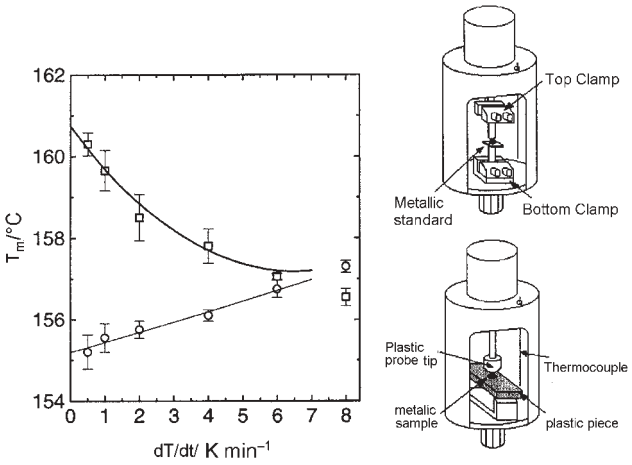

Fig. 3 Examples of temperature calibrations of the equipment. Onset temperature in the melting of an indium standard as a function of heating rate (the error bars are included). □ – extension mode; ○ – three-point bending mode. The solid lines are the second order polynomial fittings of the experimental results. The schemes of the different arrangements used for the extension (top) and the three-point bending (bottom) modes are also included

In this work calibration experiments at different heating rates were carried out using indium (true melting point 156.6°C) as the standard (from Goodfellow, 99.99999% purity), and both flexural and tensile procedures. The onset temperatures as a function of the heating rate are depicted in Fig. 3. The results were fitted with a 2nd order polynomial up to the heating rate of 6°C min^{-1}. The flexural results show an expected heating rate dependence, that is also seen in typical calibration experiments in DSC [27]: the onset temperature decreases almost linearly with decreasing heating rate. However, an opposite tendency is seen for the tensile calibrations and no linear relationship was detected. This could be a consequence of the more complex thermal environment underwent by the standard with this arrangement. Isochronal DMA experiments were also performed at 1 Hz on a poly(methyl methacrylate) film (from Goodfellow) and it was detected a decrease of the temperature of the maximum loss modulus as the heating rate increases. This behaviour is in agreement with that detected using indium.

The results at 4°C min^{-1} may be directly used for correcting the temperature of the TSR result on heating. The temperature read during the isothermal creep stage of the TSR experiment (T_σ) may be corrected using the extrapolated values of the graphics in Fig. 3 for a zero heating rate.

Note that, in principle, one should use more than one standard for correcting the temperature axis because the temperature lag (difference between the true temperature of the sample and the temperature read by the sensor) varies probably along the temperature axis. Moreover, the used procedure for calibration does not account for the thermal resistance of the sample. In fact, the use of metallic standards as proposed here, that have high

thermal conductivity, mainly corrects the temperature that is located near the surface of the sample. Routines including the location of a second thermocouple in different positions inside the sample could bring new insights about this effect.

Sensitivity of the temperature programs and removal of the thermal expansion effects

The good sensitivity/control and reproducibility of the temperature program are important to warrant reliable results. Figure 4 shows an example of a temperature program for a TS experiment. The temperatures are those read by the sensor located in the furnace, with no further corrections. Two equal and consecutive experiments are presented in Fig. 4. The two traces match almost perfectly indicating a good reproducibility of the experimental set-up.

Figure 4 shows that the temperature *vs*. time plot during the creep stage is quite horizontal. Moreover, the first descending of temperature starts abruptly as well as the second one (after a decrease of ΔT_w=3°C, as programmed). The imposed scanning rate for the final heating was 4°C min^{-1} that corresponds to the slope of the *T*–*t* plot shown in Fig. 4.

This temperature program was used to obtain TS data for a poly(methyl acrylate), PMA, cross-linked with 0.1% of ethyleneglycol dimethacrylate, EGDMA. More details about the preparation of this sample were reported in [28]. A TS experiment with T_σ=30°C is shown in Fig. 5, where the strain is represented both *vs*. time (Fig. 5a) and temperature (Fig. 5b). The drop of ε(*T*) during the recovery process starts typically some 20 degrees below T_σ. One should then expect a plateau in ε(*T*) well before the recovery process, and a recovery tending to ε=0 for temperatures above the relaxation. The rough data do not present such tendency, but rather a continuous increase of ε both in the low (below 15°C) and high (above 35°C) temperature regions of the TS experiment. This is due to the fact that during the temperature variations the geometry of the sample was also changing according to its thermal ex-

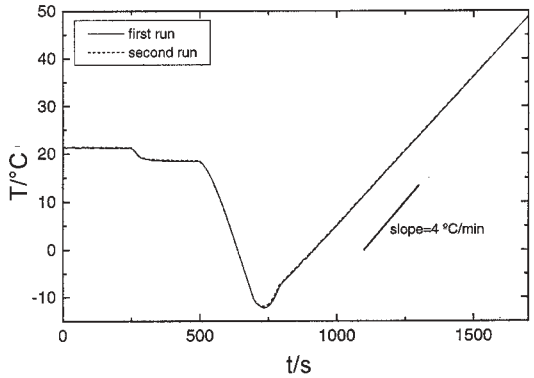

Fig. 4 Sensor temperature for two consecutive runs with the same TS program: T_σ=30°C, ΔT_w=3°C, T_o=–5°C, t_σ=t_r=4 min and β=4°C min^{-1}

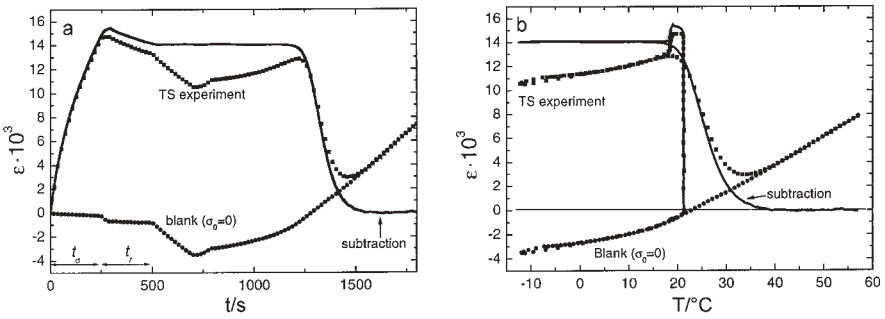

Fig. 5 Strain *vs*. time a – and temperature b – for a TS experiment on a PMA crosslinked with 0.1% EGDMA (squares). It is also presented the corresponding blank experiment (circles) and the subtraction of the two curves (solid line). The used creep stress was σ_0=0.08 MPa and the other conditions are the same of Fig. 4

pansion coefficient. Moreover, even some parts of the equipment (for example the clamps or the bending platform) may undergo some geometrical changes that will be included in the measurement of the sample's strain.

Therefore, in some cases it may be necessary to perform 'blank experiments' in order to eliminate such thermal expansions effects [14]. A blank experiment should be carried out under the same experimental parameters of the TS experiment under study but with no employment of a creep stress. Such kind of blank experiment is also shown in Fig. 5. It contains all the changes in the sample's geometry not resulting from the recovery process under study. The subtraction of the two curves gives a TS curve exhibiting the expected appearance.

Note that for the case shown in Fig. 5 the running of a blank experiment was necessary. In some cases analysed in our laboratory such procedure was found to be negligible.

Results and discussion

TSR, TSCreep and TS experiments were carried out on a thermoset synthesized from a polyester resin based on orthophthalic acid. More details on this material can be found in [16]. Figure 6 shows a $|d\varepsilon/dt|/\sigma_0$ *vs*. *T* plot of the results obtained using a flexural mode in the glass transition region. Note that the apparatus measures ε *vs*. *T*. The derivative of the strain was obtained numerically. It is important to note that the global TSR and TSCreep results exhibit clear peaks that allow to identify the glass transition of the material, more difficult to detect using DSC [16, 17]. The TSR and TSCreep techniques may be considered a useful tool to determine the glass transition temperature of polymeric materials. However, global experiments displaying the overall glass transition relaxation may be performed mainly in thermosets, composites or semi-crystalline polymers. For amorphous polymers, irreversible flow above

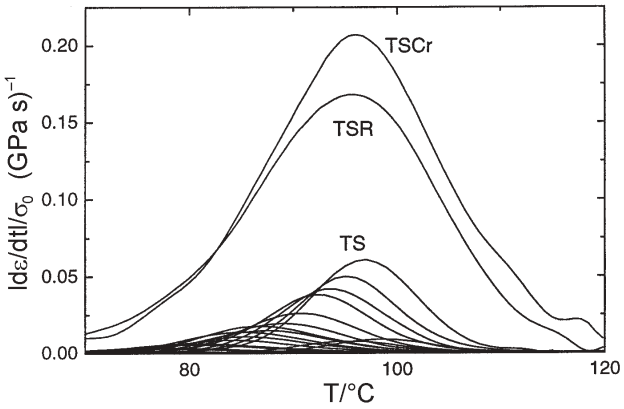

Fig. 6 $|d\varepsilon/dt|/\sigma_0$ *vs*. *T* plot for a polyester resin in the glass transition region, corresponding to TSR, TSCreep and TS experiments. Experimental conditions for the TSCreep and TSR experiments: T_0=30°C, σ=0.1 MPa and β=4°C min^{-1}. Experimental conditions for the TS results: T_σ varied between 56.4 and 93°C, σ=1 MPa, ΔT_w=3°C, t_σ=t_r=4 min, T_0=30°C and β=4°C min^{-1}

T_g prevents the running of global TSR experiments with creep temperatures well above T_g.

Figure 6 shows that the information given by global TSR or TSCreep experiments is formally the same. For example, the temperature corresponding to the maximum of both two peaks is the same. The contour of the TS experiments follows the global curves, as expected and observed in TSDC experiments [29–31].

Determination of the thermokinetic parameters in TS experiments

In a simple analysis, each TS curve can be analysed as a thermally stimulated mechanical recovery process of an elementary mechanism. The Voigt–Kelvin model can be used in order to predict the dependence of the strain on time or temperature. The corresponding constitutive equation is:

$$\tau(T)\frac{d\varepsilon(t)}{dt}=\frac{\sigma_0}{E}-\varepsilon(t) \tag{1}$$

where σ_0 is the static strain, *E* is the Young modulus of the spring element and $\tau(T)$ is the retardation time of the process.

The characteristic time is $\tau=\eta/E$, where η is the viscosity of the Newtonian dashpot which is in parallel with the elastic element. This model is equivalent to the Debye model used in the TSDC technique. Applying Eq. (1) to a mechanical recovery process (σ_0=0) during heating at a constant rate $\beta=dT/dt$, the temperature dependence of the strain is

$$\varepsilon(T)=\varepsilon_0\exp\left[-\frac{1}{\beta}\int_{T_0}^{T}\frac{1}{\tau(T')}dT'\right] \tag{2}$$

where $\varepsilon_0=\varepsilon(T_0)$.

The creep rate $d\varepsilon/dt$ can be written as:

$$\frac{d\varepsilon}{dt}=-\varepsilon_0\tau^{-1}(T)\exp\left[-\frac{1}{\beta}\int_{T_0}^{T}\frac{1}{\tau(T')}dT'\right] \quad (3)$$

It can be easily found from Eqs (2) and (3) that

$$\tau(T)=-\frac{1}{\beta}\frac{\varepsilon(T)}{d\varepsilon(T)/dT} \quad (4)$$

Equation (4) is often used for calculating the temperature dependence of the retardation time directly from the experimental results, allowing to have a picture on the molecular mobility involved in this temperature and time scale range. This procedure, often called Bucci or BFG method, was first derived for the treatment of TSDC data [32]. The calculation of $\tau(T)$ by the BFG method is carried out between $\sim T_{max}$–30 and $\sim T_{max}$, where T_{max} is the temperature of the maximum absolute creep rate. In complex systems, no experimental TS curve arises from a pure elementary process, but rather involves the response of a distribution of retardation times. Due to this fact, the $\tau(T)$ values calculated with Eq. (4) deviate from the real mean retardation time, mainly for temperatures above T_{max} [11–13]. Moreover, the relaxation times range is not significantly increased by the use of temperatures above T_{max} because $\varepsilon(T)/[d\varepsilon(T)/dT)]$ does not vary too much above the inflexion of $\varepsilon(T)$.

The range of the retardation times of a typical TS curve acceded by the BFG method is usually less than 2 decades. Therefore the corresponding $\tau(T)$ plots rarely show the Vogel character and even close to T_g they are fitted with the Arrhenius equation:

$$\tau(T)=\tau_0\exp(E_a/RT) \quad (5)$$

where τ_0 its a pre-exponential factor, E_a is an apparent activation energy and R is the gas constant. This equation is easily linearized and, from the $\tau(T)$ data calculated by the BFG method, the two Arrhenius thermokinetic parameters of each TS experiment are obtained by linear regression.

As an example, several TSR flexural experiments were carried out in a semicrystalline poly(ethylene terephthalate), PET. The samples were prepared from a 1 mm thick PET bar (Goodfellow – catalogue number ES303010), previously annealed at 163°C for 1 h to induce crystallinity. More results on this material are discussed in the second part of this work [33]. Some Arrhenius lines of TS experiments on this PET obtained at different T_σ in the glassy state, but close to T_g, are shown in Fig. 7.

The Arrhenius lines tend to converge on a single point (at higher temperatures and lower retardation times). This effect, often called compensation phenomenon, has been extensively discussed in the literature and is always observed in the glass transition of glass-forming substances studied by TSR or TSDC.

Figure 7 shows that the BFG method leads to nearly perfect linear $\ln\tau$ *vs.* $1/T$ relationships (correlation coefficients better than 0.997). This should be a sufficient condition for using this method on the data treatment. Repetition of a same experi-

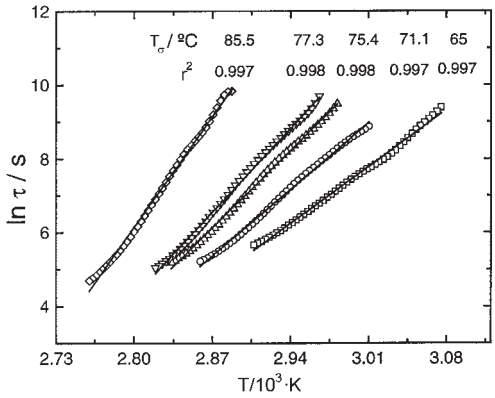

Fig. 7 Arrhenius plots for some TS data in the glass transition region of a semicrystalline PET bar. The creep temperatures, T_σ, are indicated in the figure. The relaxation times were calculated by the BFG method. The experimental conditions were: σ_0 between 8 and 20 MPa, depending on T_σ, ΔT_w=3°C, T_0 was typically 40°C below T_g, t_σ=t_r=4 min and β=4°C min^{-1}

ment at different days, carried out with T_σ=85.5°C and under the same other experimental conditions of those in Fig. 7, lead to the following activation energies: 357.2, 343.5, 345.0 and 353.6 kJ mol^{-1}. These experiments suggest an error on the calculation of the activation energy of ca 5–10% due to experimental factors affecting the reproducibility of TSR tests.

Another possibility of obtaining the thermokinetic parameters is to fit directly the data according to Eq. (2). Such procedure was previously used on a polycarbonate system [15]. Three parameters are obtained for each TS curve: E_a, τ_0 and ε_0. Initial approximations of the ε_0 values are given by the $\varepsilon(T)$ values in the higher plateau of the experimental TS curves. The three adjustable parameters are obtained by minimization of

$$S=\sum_i[\varepsilon(T_i)-\varepsilon(T_i,\tau_0,E_a,\varepsilon_0)]^2 \quad (6)$$

where $\varepsilon(T_i)$ are the experimental values and $\varepsilon(T_i, \tau_0, E_a, \varepsilon_0)$ are the theoretical ones obtained through Eq. (2). The fitting was conducted for values of $\varepsilon(T)$ between the initial higher plateau and approximately the temperature at the inflexion of the curve, covering typically a temperature range between 20–40°C.

Some TS experiments on the PET previously mentioned were carried out at T_σ=68.7°C. However, in this case the sample was aged at that temperature during different ageing times, t_a, before the beginning of the TS experiment. The purpose of this kind of study is to investigate the influence of physical ageing on the TS results [17]. The residues computed through Eq. (6) were obtained from a single TS experiment, carried out after t_a=235.4 min, and plotted in Fig. 8 for a large set of E_a and logτ_0 pair of values.

It is interesting to note that the shape of the residues plot in Fig. 8 is similar to a valley. If we fix E_a or $\log\tau_0$ and follow the evolution of S as a function of the other parameter, we should pass through a minimum of S. Such behaviour was observed in all residues plot, computed from the TS curves on the same PET performed at other creep temperatures. Even in other materials the same shape for such residues plot for TS experiments was observed. Also, in TSDC experiments this valley shaped residues plot was observed. This is a result of an intrinsic compensation of the E_a and $\log\tau_0$ parameters in Eq. (2). Assuming we have a pair of (E_a, $\log\tau_0$) that represents well an experimental curve, if we change, for example, E_a we can find a new $\log\tau_0$ that minimises again S and eventually seems to reproduce again the experimental data. In a first analysis, this compensation effect suggests that the determination of the thermokinetic parameters of TS experiments is an ill-posed problem. However, Fig. 8 shows clearly that an absolute minimum of S is found in the (E_a. $\log\tau_0$) plane. Those thermokinetic parameters could be considered the ones that better describe the TS experiment. For the specific example of Fig. 8 the minimum is found when E_a=175.6 kJ mol^{-1} and $\log\tau_0$=–23.8 s.

Figure 9 shows experimental results obtained in semicrystalline PET at T_σ=68.7°C after different annealing times: 3.4, 10.4, 55.4 and 235.4 min. The obtained activation energies, using the direct fitting method are 218.4, 210.0, 190.2 and 175.6 kJ mol^{-1}, respectively. The simulations of the theoretical curves, computed with the fitted thermokinetic parameters, are also shown in Fig. 9. They agree with the experimental data up to the inflexion of the curves. The decrease of both E_a and ε_0 with increasing ageing time was also observed in a thermoset system [17]. Thus the results reported here strengthen the universality of the discussion and conclusions presented in the work reported in [13].

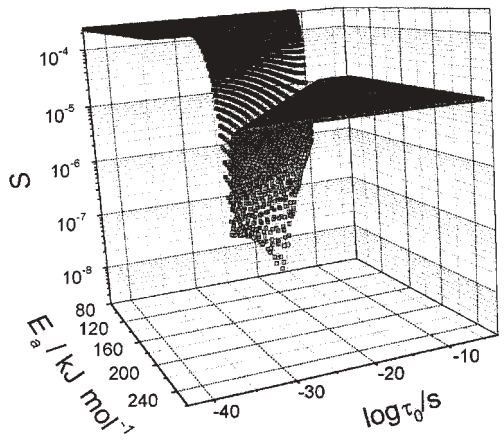

Fig. 8 Residues as a function of the thermokinetic parameters using Eq. (6) on a TS experiment obtained with the same PET of Fig. 7, aged during 235.4 min at 68.7°C prior the TS experiment. We used T_σ=68.7°C, σ_0=20 MPa and the other experimental conditions were the same as in Fig. 7

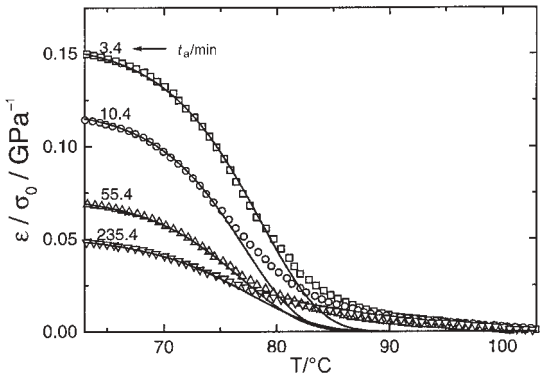

Fig. 9 Normalised strain *vs*. temperature for the same PET of Fig. 7 aged during distinct times (t_a) at 68.7°C before the TS experiments. The experimental conditions were the same as in Fig. 8. Solid lines: theoretical curves describing the experimental results using parameters obtained by the direct fitting method (minimisation of Eq. (6)). Note that many experimental points are skipped for better comparison with the fitted curves

Another procedure that allows for the calculation of the thermokinetic parameters, which has been proposed for the TSDC technique, is the initial-rise method [34]. It is based on the fact that well below T_{max} the variation of the creep rate, $d\varepsilon/dt$, given by Eq. (3), is mostly affected by the $\tau^{-1}(T)$ term, i.e., the exponential term can be considered as constant. Taking the Arrhenius behaviour, one can write, under this assumption:

$$d\varepsilon/dt \sim -\exp(-E_a/RT) \tag{7}$$

From Eq. (7) one can extract E_a from the slope of the linear regression of $\ln(-d\varepsilon/dt)$ *vs*. $1/T$. The pre-exponential factor, τ_0, may be obtained form the relationship between E_a, τ_0 and T_{max}:

$$\tau_0 \exp\frac{E_a}{RT_{max}} = \frac{RT_{max}^2}{\beta E_a} \tag{8}$$

This equation was obtained by calculating the temperature of the maximum of the absolute creep rate variation by differentiation of Eq. (3).

An example of using this method for some TS experiments in the glass transition region of the same PET studied before (Fig. 7) is shown in Fig. 10.

The $\ln(-d\varepsilon/dt)$ *vs*. $1/T$ lines of all experiments present good linearity. In this case, for each experiment, we used the data ranging from temperatures at which the strain rate is ca $(d\varepsilon/dt)_{max}/20$ and $(d\varepsilon/dt)_{max}/5$, where $(d\varepsilon/dt)_{max}$ is the maximum strain rate (that occurs at $T=T_{max}$). Outside this data range it was observed a deviation from linearity. Note that as we are approaching $(d\varepsilon/dt)_{max}$ the initial assumption of this method is no further valid. The selected data range is in agreement with the data

ranges used in other works [35], where the activation energies of TSDC results were obtained by this method.

Figure 11 shows the activation energy of several TS experiments of PET as calculated by the three methods: BFG, direct fit and initial-rise methods. All the results are in good agreement, thus indicating that Eq. (2) supplies a good description of the thermally simulated behaviour of quasi-elementary process, at least up to temperatures close to T_{max}.

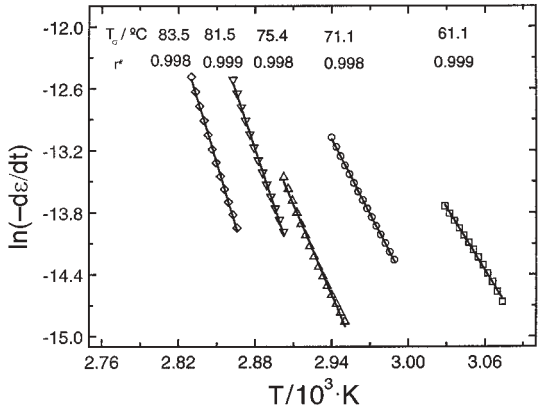

Fig. 10 Derivative of strain (t in seconds) *vs*. reciprocal temperature for the same PET of Fig. 7 in order to use the initial rise method. The experimental conditions were the same as in Fig. 7

Other methods may be used for obtaining the thermokinetic parameters. By following the T_{max} values of the TS curves obtained at different heating rates, the plot $\ln(T_{max}^2/\beta)$ *vs*. $1/T_{max}$ allows to calculate the activation energy; Eq. (8) may be again directly used for the calculation of τ_0. The disadvantage of this method is the need for several experiments at different heating rates, which is time consuming and associates problems of temperature calibration. Finally, it is worth to be noted that there are also methods that allow for the calculation of the activation energy of a TS experiment based on the shape of the curve $-d\varepsilon/dt$ *vs*. $1/T$ [36]. A disadvantage of such methods is that a very limited number of points of the curve are used.

Conclusions

This work has demonstrated that a commercial DMA/TMA apparatus (specifically a Perkin Elmer DMA7 equipment) can be used to carry out global TSR and TSCreep and TS experiments, with a good temperature control. This has obvious advantages for comparing such results with dynamic data under the same thermomechanical environment. The temperature calibration may be an important procedure to be taken into account and any calibration routine should depend on the mechanical mode used. It was also shown that performing previous blank experi-

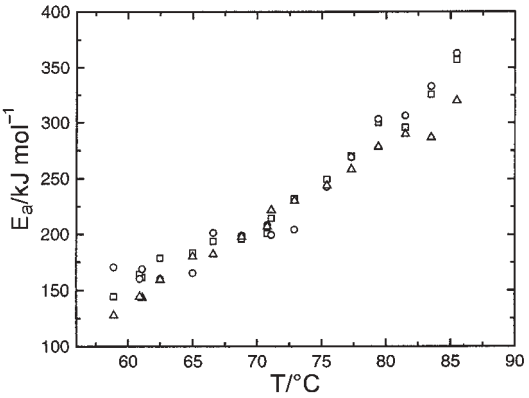

Fig. 11 Activation energy *vs*. temperature for the same PET of Fig. 7 in the glass transition region. The activation energies were calculated by different methods. Squares: BFG method; triangles: direct fit; circles: initial rise method

ments may be required to eliminate geometrical changes not assigned to the relaxational processes under study.

Several methods for the determination of the thermokinetic parameters, and then access to the molecular mobility of the system, in TS experiments on semicrystalline PET, were discussed and compared. The obtained activation energies were found to be independent on the method used. The direct fit method pointed out to an intrinsic compensation effect between the activation energy and the pre-exponential factor in the used equation that describes the thermally stimulated recovery during heating.

* * *

NMA and JFM acknowledge the financial support of Fundação para a Ciência e Tecnologia (Project PRAXIS/P/CTM/14171/1998). Support from the Protuguese-Spanish joint research action (Spain: HP 1999-0024; Portugal: E/69/00) is also acknowledged: NMA wishes to acknowledge Fundação para a Ciência e Tecnologia for the financial support trough the grant PRAXIS XXI/BD/20327/99.

References

1 R. N. Haward and R. J. Young, (Eds.,) The Physics of Glassy Polymers, 2nd Ed., Chapman and Hall, London 1997.
2 L. Woo, S. Wesphal and M. T. K. Ling, Polym. Eng. Sci., 34 (1994) 420.
3 L. Woo, S. Wesphal, S. Shang and M. T. K. Ling, Thermochim. Acta, 284 (1996) 57.
4 R. Richert and A. Blumen (Eds.), Disordered Effects on Relaxational Processes, Springer Verlag, Berlin 1994.
5 J. van Turnhout, Thermally Stimulated Discharge of Polymer Electrets, Elsevier, New York 1975.
6 C. Lavergne and C. Lacabanne, IEEE Electrical Insulation Magazine, 9 (1993) 5.
7 C. Lacabanne, D. C. Chatain and J. C. Mompajens, J. Macrom. Sci. Phys. B, 134 (1977) 537.

8 C. Lacabanne, D. C. Chatain, J. C. Mompajens, A. Hiltner and E. Baer, Solid State Commun., 27 (1978) 1055.
9 C. Lacabanne, A. Lamure, G. Teyssedre, A. Bernès and M. Mourgues, J. Non-Cryst. Solids, 172 (1994) 174.
10 J. P. Crine, J. Appl. Phys., 66 (1989) 1308.
11 M. G. McCrum, Polymer, 23 (1982) 1261.
12 M. G. McCrum, Polymer, 25 (1984) 299.
13 M. G. McCrum, Polymer, 25 (1984) 309.
14 H. H. Y. Tang and H. L. Williams, J. Appl. Polym. Sci., 40 (1990) 495.
15 N. M. Alves, J. F. Mano and J. L. Gómez Ribelles, Macromol. Symp., 148 (1999) 437.
16 N. M. Alves, J. F. Mano and J. L. Gómez Ribelles, J. Mat. Res. Innovat., 4 (2001) 170.
17 N. M. Alves, J. F. Mano and J. L. Gómez Ribelles, Polymer, 42 (2001) 4173.
18 N. N. Peschanskaya, P. N. Yakushev, A. B. Sinani and V. A. Bershtein, Thermochim. Acta, 238 (1994) 429.
19 V. A. Bershtein, N. N. Peschanskaya, J. L. Halary and L. Monnerie, Polymer, 40 (1999) 6687.
20 B. B. Sauer, P. Avakian, B. S. Hsiao and H. W. Starkweather, Macromolecules, 23 (1990) 5119.
21 J. F. Mano; N. T. Correia and J. J. Moura Ramos, Polymer, 35 (1994) 3561.
22 J. F. Mano, Thermochim. Acta, 332 (1999) 161.
23 S. V. Shenogin, S. I. Nazarenko, S. N. Rudnev, E. F. Oleinik and G. W. H. Höhne, Vysokomol. Soedin, 39 (1997) 2087.
24 C. M. Earnest and R. J. Seyler, J. Testing and Evaluation, 20 (1992) 430.
25 C. M. Earnest and R. J. Seyler, J. Testing and Evaluation, 20 (1992) 434.
26 R. Riesen and J. E. K. Schawe, J. Therm. Anal. Cal., 59 (2000) 337.
27 G. W. H. Höhne, W. Hemminger and H.-J. Flammershein, Differential Scanning Calorimetry – An Introduction for Practitioners, Springer Verlag, Berlin 1996.
28 J. M. Cuesta Arenas, J. F. Mano and J. L. Gómez Ribelles, J. Non-cryst. Solids, accepted.
29 J. F. Mano and J. J. Moura Ramos, J. Thermal Anal., 44 (1995) 1037.
30 J. F. Mano, N. T. Correia, J. J. Moura Ramos, S. R. Andrews and G. Williams, Liquid Crystals, 20 (1996) 201.
31 N. Tsutsumi and Y. Okabe, J. Polym. Sci.: Polym. Phys., 38 (2000) 88.
32 C. Bucci, R. Fieschi and G. Guidi, Phys. Rev., 148 (1966) 816.
33 N. M. Alves, J. F. Mano and J. L. Gómez Ribelles, Polymer, accepted.
34 S. H. Carr, in Electric Properties of Polymers, Ed. D. A. Seanor, Academic Press, New York 1982.
35 R. Chen and G. A. Haber, Chem. Phys. Lett., 2 (1968) 483.
36 K. Marossy, G. Deak, S. Kéki and M. Zsuga, Macromolecules, 32 (1999) 814.